Available online at www.sciencedirect.com

SciVerse ScienceDirect

Advances in Space Research 51 (2013) 2297–2308

ADVANCES IN SPACE RESEARCH (a COSPAR publication)

www.elsevier.com/locate/asr

Satellite derived aerosol optical depth climatology over Bangalore, India

V. Sreekanth *

Department of Physics, CMR Institute of Technology, Bangalore 560 037, India

Received 2 May 2012; received in revised form 3 December 2012; accepted 16 January 2013
Available online 4 February 2013

Abstract

Climatological aerosol optical depths (AOD) over Bangalore, India have been examined to bring out the temporal heterogeneity in columnar aerosol characteristics. AOD values at 550 nm derived from the Moderate Resolution Imaging Spectroradiometer (MODIS) sensor onboard NASA's Terra and Aqua satellites, for the period of 2002–2011 have been analyzed (independently) for the purpose. Frequency distributions of the AOD values are examined to infer the monthly mean values. Monthly and seasonal variations of AOD are investigated in the light of regional synoptic meteorology. Climatological monthly and seasonal mean Terra and Aqua AOD values exhibited similar temporal variation patterns. Monthly mean AOD values increased from January, peaks during May and thereafter (except for a secondary peak during July) fall off to reach a minimum during December. Monsoon season recorded the highest climatological seasonal mean AOD, while winter season recorded the lowest. AOD values show an overall increasing trend on a yearly basis, which was found mainly due to sustained increase in the seasonal averaged AOD during summer. The results obtained in the present study are compared with that of the earlier studies over the same location and also with AOD over various other Indian locations. Finally, the radiative and climatic impacts are discussed.

Keywords: MODIS; Aerosol optical depth; Temporal variation

1. Introduction

The rapid urbanization of the world countries not only poses the health and socio-economic challenges, but also deep environmental concerns such as water and air quality (Guinot et al., 2007). Air quality is mainly dominated by atmospheric aerosols. Apart from air quality, aerosols through their direct and indirect effects have the potential to perturb the Earth-atmosphere energy (in terms of incoming and outgoing radiation) balance (Charlson et al., 1992). Studies have shown that aerosols can also affect the atmospheric general circulation patterns (Lau et al., 2006) and biochemical cycling (Xin et al., 2005). Regional distributions of aerosols, their inter-annual variability and detailed descriptions of spectral aerosol optical properties are needed in order to understand the influences of aerosols on the climate of the region (Eck et al., 2001). In the health perspective, a very recent study by Dimitrova et al. (2012) has shown a statistically significant correlation between the increase of asthma attacks in children and elevated concentrations of aerosols of diameter 10 μm and less (PM10) for metropolitan Phoenix, Arizona. Characterization of the aerosols becomes an increasingly challenging task due to their spatio-temporal variability in terms of abundance, optical, physical and chemical properties. This calls for highly resolved aerosol measurements in space and time over the globe. In this regard, a number of ground-based aerosol networks were established worldwide, procuring continuous data sets on a variety of aerosol parameters over land and even over oceans (e.g. AErosol RObotic NETwork (AERONET); Holben et al., 1998; Smirnov et al., 2009). All these efforts might often suffer from the technical snags in the instrumentation, lack of manpower and proper maintenance which can eventually result in gaps in the valuable database. The emerging capability of satellite remote sensing provides an unprecedented opportunity to advance the understanding of aerosol-air

* Tel.: +91 80 41303701.
E-mail address: sree_hcu@yahoo.co.in.

0273-1177/$36.00 © 2013 COSPAR. Published by Elsevier Ltd. All rights reserved.
http://dx.doi.org/10.1016/j.asr.2013.01.022

quality-climate linkages (Yu et al., 2010). Operational remote sensing of aerosols from satellites provides an efficient means to achieve a global and temporal characterization of aerosols. Satellite sensors view the entire earth and produce global images, thus resolving the spatial patterns resulting from the spatial inhomogeneities (Remer et al., 2005). The current study employs a climatological database on aerosol optical depths from the passive Moderate Resolution Imaging Spectroradiometer (MODIS) sensor.

Southern Asia, extending from Pakistan and Afghanistan to Indonesia and Papua New Guinea, is one of the most heavily populated regions of the world (Lawrence and Lelieveld, 2010). India, one of the densely populated and developing countries (in terms of urbanization and industrialization) in Asia, with diverse geographic and climatic conditions, living and cooking habits, can be a potential source region for a wide variety of aerosols. The current study focuses on the long-term temporal variation of AOD over Bangalore (BNG, 13°N, 77.5°E, 920 m asl), India, derived from the MODIS sensor. Very few studies on aerosol optical properties (Ramachandran and Cherian, 2008; Vinoj et al., 2004, 2009; Ramachandran et al., 2012) were conducted earlier over BNG, which is the third most populous metropolitan city and fifth most populous urban agglomeration in India. Some of the previous studies on aerosol characterization over BNG include (i) estimation of aerosol radiative forcing (Babu et al., 2002); (ii) seasonal heterogeneity in the vertical distribution of aerosols using micro pulse LIDAR (Satheesh et al., 2006); (iii) observation of elevated aerosol above reflecting clouds (Satheesh et al., 2008); (iv) observation of discrepancies between measured and modeled aerosol radiative effects (Satheesh et al., 2010). All the earlier studies on AODs were limited to either small data sets or narrow statistical analysis. In the present study a comprehensive investigation on the climatological picture of the temporal variation of AOD has been attempted. The AOD values obtained over BNG were compared with that of other parts of India.

2. MODIS sensor and database

The AOD data (at 550 nm) used for analysis in the present study are a part of MODIS Terra (MOD08_D3) and Aqua (MYD08_D3) level-3 1° x1° Collection 5 (C005) daily gridded atmospheric data product and are acquired from the website www. http://gdata1.sci.gsfc.nasa.gov. The first MODIS instrument was launched onboard the Terra satellite on 18 December 1999, with daytime equator crossing at 1030 LT, as part of the NASA's Earth Observing System (EOS) mission and the second one on 4 May 2002 onboard the Aqua platform with daytime equator crossing at 1330 LT. These are uniquely designed (wide spectral range, high spatial resolution, and daily global coverage) to observe and monitor the changes in the Earth's atmosphere. MODIS with its 2330 km viewing swath provides daily global coverage. Since February 2000, MODIS has been continuously acquiring measurements at 36 spectral bands between 0.415 and 14.235 μm with spatial resolution of 250, 500 and 1000 m. The retrieval of aerosol data by MODIS is performed with special algorithms (e.g. Tanré et al., 1997; Kaufman et al., 1997; Levy et al., 2003, 2007; Remer et al., 2005), which are different over land and ocean because of differences in their surface characteristics. MODIS Collection 5 data set is an improvement over earlier collections, generated with upgraded algorithm (Remer et al., 2005; Remer et al., 2008). These improvements include incorporation of polarization information in the radiative transfer calculations as well as more realistic aerosol models for different parts of the globe. The accuracy of satellite estimates of AOD was first suggested based on theoretical analyses (Kaufman et al., 1997). Over the land, the MODIS-derived AODs are validated against the in situ AOD observed at AERONET stations, which shows that AOD retrievals in the visible wavelengths are generally within the pre-launch uncertainty (Jethva et al., 2007; Remer et al., 2008). Over India, MODIS derived AOD (Collection 5) has been validated against AERONET observations over the urban location Kanpur (26.4°N, 80.3°E) in the Indo-Gangetic plains by Choudhry et al. (2012). Their results show that MODIS retrievals are will within the pre-launch uncertainty. MODIS AOD for the period January 2002 to December 2011 (10 years) has been examined in the current study to delineate the temporal variations of AOD over BNG in light of regional anthropogenic activity, synoptic meteorology and long-range transport. The data grid has been chosen to be 12.5–13.5°N and 77–78°E, BNG being located at the centre of the grid. The geographical location of BNG (solid star) is shown in Fig. 1 along with the location of other Indian sites (open circles), over which the AOD data has been compared to that of BNG.

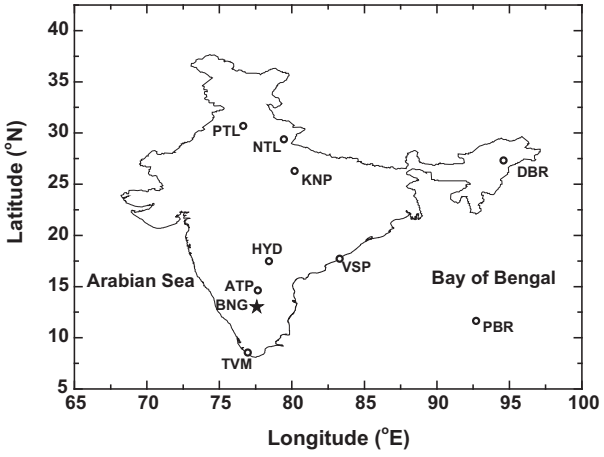

Fig. 1. Geographical location of Bangalore (solid star) along with other Indian sites (open circles) over which the AOD data has been used for comparison study.

3. Site description and synoptic meteorology

BNG, located in the Deccan plateau of south central peninsular India at an altitude of ~920 m amsl, is the third most populous city in India and the 28th most populous city in the world. With an estimated population of 8.5 million (according to 2011 population census of India), BNG is one of the fastest growing metropolis in India. The city has a very large vehicular population of ~3 million among which the motorized 2-wheelers are the main growth category. The city has an international airport, six railway stations, and seven major bus stations. They constitute a major source of anthropogenic emissions. Apart from the vehicular contribution, BNG has 13 industrial areas, among which, Peenya industrial area is considered to be one of the largest industrial areas in Asia. These industrial areas are known for manufacturing of engineering and electrical goods, textiles, hydraulics, machine tools, carbon and graphite products. By and large, the aerosol load over BNG is mainly dominated by anthropogenic activities, modulated by local meteorological conditions.

As BNG is located at an altitude of ~920 m asl, the prevailing synoptic meteorology is important in understanding the aerosol characteristics, transport mechanism and source apportionment. The climate of BNG is basically dry tropical savannah type. The climatological monthly mean temperature, relative humidity (RH in%) and monthly accumulated rainfall (in mm) are shown in the top and bottom panels of Fig. 2 respectively. April, with a monthly mean temperature ~28 °C is the warmest month; December is the coldest with mean temperature ~21 °C. RH varied almost inversely with temperature, March being the driest month with a value of ~45%. The average annual temperature is ~24 °C, RH ~65%, total annual rainfall of ~970 mm with a total number of 60 rainy days per year. The climatological mean rainfall pattern shows that considerable rain starts in May and peaks in September (~195 mm). Based on the above factors, the calendar months are grouped into four distinct seasons (Satheesh et al., 2006) viz. winter (November–February), summer (March–May), monsoon (June–August) and post-monsoon (September–October). During winter, the temperature varies from a minimum value of ~16 to a maximum of ~27.7 °C, with a diurnal mean of ~22 °C. Very little rainfall of ~77 mm (7.8% of total annual rainfall) occurs in this season and RH remains ~50–70%. Summer season is the hottest and driest season with temperature values going up to ~33 °C and mean RH values ~50%, with a minimal precipitation of ~152 mm. Monsoon and post-monsoon months are characterized by moderate temperature (monthly mean temperature ~24 °C), maximum RH values (~75%) and with total rainfall ~700 mm. Winds are mostly westerly or easterly depending on season (see Fig. 7). More details on BNG site description and local meteorology can be found in Satheesh et al. (2010).

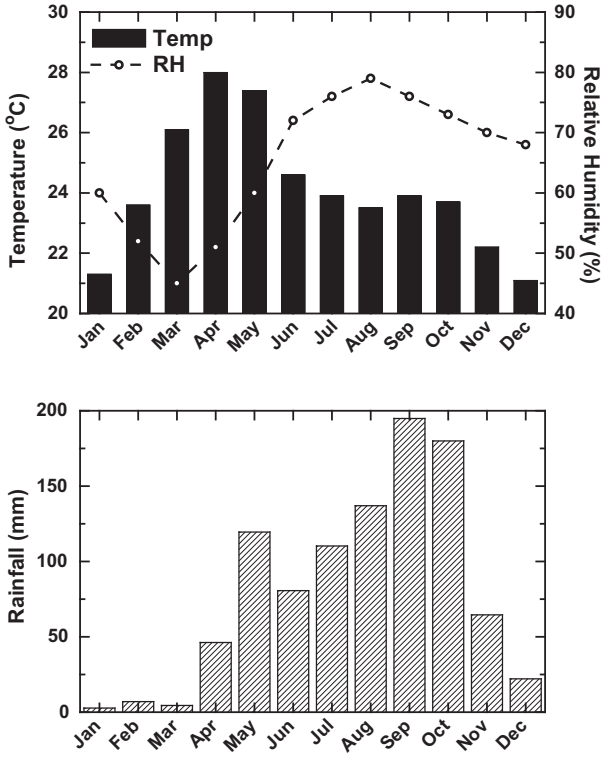

Fig. 2. (top panel) Climatological monthly mean variation of ambient air temperature (vertical column graph) and relative humidity (open circle + dashed line); (bottom panel) monthly accumulated rainfall.

4. Results and discussion

4.1. Frequency distributions of AODs

Ten years Terra AOD values are grouped into calendar months and their frequency distributions (in terms of percentage occurrence) are shown in Fig. 3. Size of the each bin is taken as 0.1. During January month, the occurrence of lower values (<0.1, first bin) of AOD is almost ~38% and the percentage occurrence decayed exponential towards the higher AOD values. The occurrence of AOD values above 0.6 is almost negligible. During February also, the pattern remained same, but the decay is slower compared to that of January. Towards summer months (March–May), the distribution is wider and a mode built up is clear with the maximum occurrence of AOD values shift toward relatively higher values around 0.2–0.5 (~50–60%). During the monsoon months (June–August), widest distributions are observed. During post-monsoon months (September and October), skewed distributions (skewed towards occurrence of higher AODs) are observed. Again, towards winter months (November, December) the distribution becomes highly skewed and finally transformed into an exponential decay form by January. The occurrence of AOD values in the lowest bin (bin-centre of 0.05) peaks in December/January and decreases through summer and monsoon months and retreats towards post-monsoon and winter months. The occurrence of the relatively higher values (>0.6) of AOD

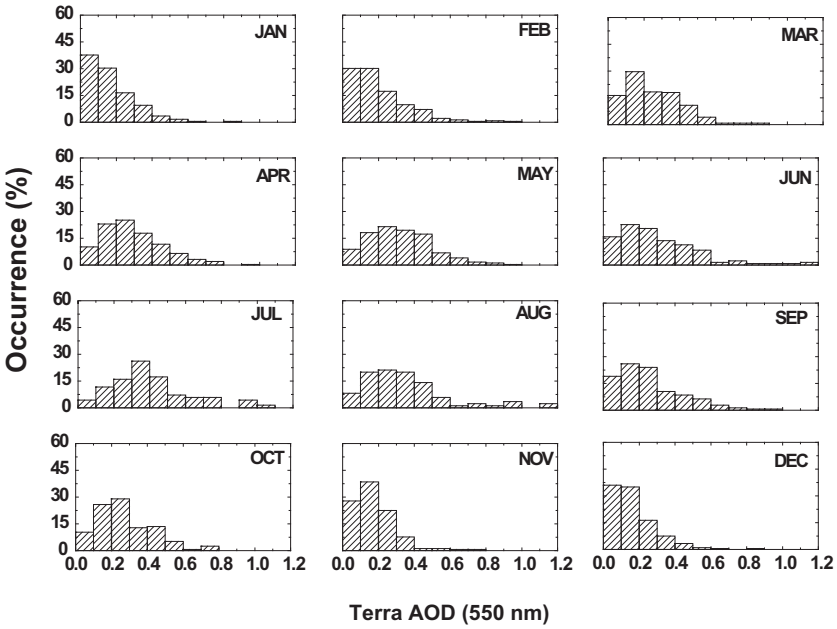

Fig. 3. Month-wise occurrence frequency distribution of the AODs for the study period.

peaks in monsoon months and almost negligible in other seasons. Frequency distribution of Aqua AOD values (not shown) also exhibited similar pattern for all the months.

4.2. Monthly variations

Monthly mean variation of the AOD (Terra and Aqua) values for the study period is shown as a box and whisker plot in Fig. 4. In Fig. 4, solid dots indicate the mean values; the range of the box indicates the 25 and 75 percentile values; centre line indicates the 50 percentile value (median); the range of the whiskers indicates the standard deviation of the mean value; dashes and crosses indicate the minimum, maximum values and the 1, 99 percentile value of the dataset for the particular month. The monthly mean AOD values along with other statistically meaningful parameters are given in Table 1. Each of the months mean value has been deduced from statistically significant number of daily AOD values. Only during July and August the dataset has fewer points (less than 100) due to the frequent spells of rainfall and cloudy skies.

From Fig. 4 the following gross features are evident (1) both Terra and Aqua monthly mean AOD values and their statistics exhibited similar temporal pattern; (2) the mean AOD value is always higher than that of median throughout the year; (3) mean AOD value increased up to May, a dip in June and a secondary peak during July and thereafter decreased towards winter months; (4) the spread in values (in terms of the standard deviation) is highest in July and least during December; (5) highest AOD values are recorded during June–August and the least value is almost same for all the months.

Terra (Aqua) AODs with a mean value of $\sim 0.170 \pm 0.13$ (0.145 ± 0.12) during January, increased towards summer months and the annual peak of $\sim 0.4 \pm 0.23$ (0.474 ± 0.23) has been recorded during July. The values after the $\pm$ symbol represent the standard deviation. From July through December the values dropped off and reach a least value of $\sim 0.16 \pm 0.12$ (0.146 ± 0.1). Note that the values in the parenthesis correspond to Aqua. The mean values are consistently high compared to the median (50 percentile), which suggests that the distribution of the frequency occurrence is always skewed towards the higher values. The monthly mean AOD pattern observed in the present study is very much in line with that of Vinoj et al. (2009) for the wavelengths greater than 500 nm. Their results are based on the ground-based point measurements using a multi-wavelength radiometer for the period 2001–2005. The increase in mean AOD towards the summer months (March–May) can be attributed to the dry weather conditions (Fig. 2). The wet removal processes become insignificant during these months due to scanty rainfall conditions. During these months the solar heating and length of the daytime will be maximum, resulting in the strong turbulent mixing and convective motions, lifting of aerosols from the surface. This mechanism is also evident from the summer time vertical aerosol extinction profiles examined by Satheesh et al. (2006) using a micro pulse LIDAR over BNG. They observed cloud like structures within the aerosol layers during summer due to intense convective mixing of aerosols. All these processes enhance the AOD values during this season. The monsoon months AOD values are moderate with a peak in July. From Fig. 3 it is clear that the occurrence percentage of higher AOD values (>0.6) is more in July and August compared to other months, which might have influenced the mean value. Also, the decrement in the AOD value due to the washout of aerosols by rainfall might has compensated by the hygroscopic growth of the aerosols. Note that the ambient RH

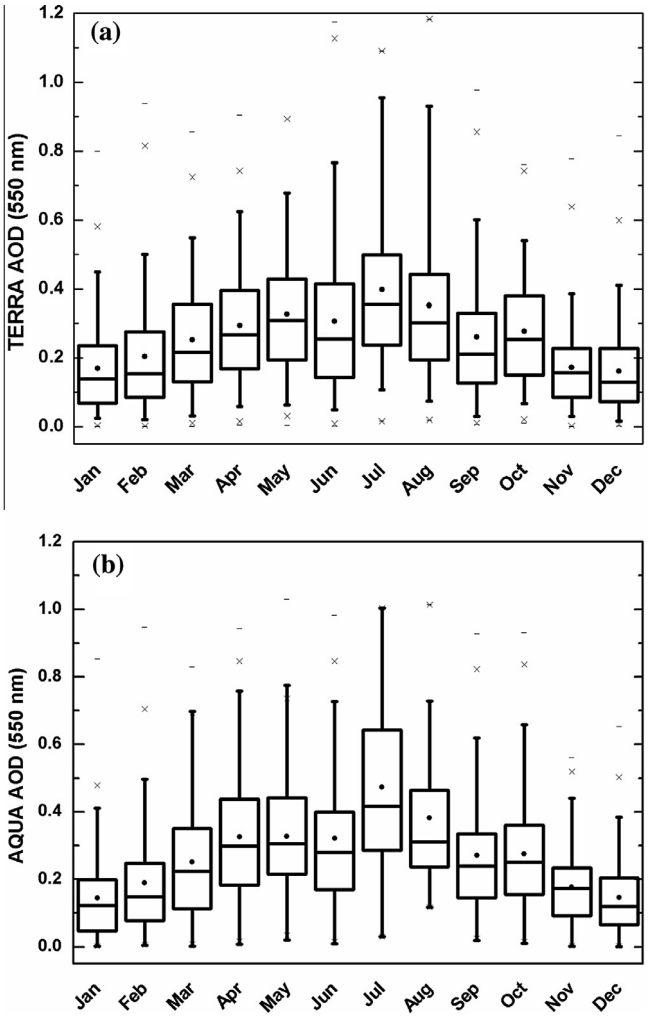

Fig. 4. Box and whisker plot for the monthly mean variation of (a) Terra AOD; b) Aqua AOD. Solid dots indicate the mean values. The range of the box indicates the 25 and 75 percentiles values; centre line indicates the 50 percentile value. The range of the whiskers indicates the standard deviation of the mean value. Dashes indicate the minimum, maximum values. Crosses indicate 1, 99 percentiles value of the dataset for the particular month.

value becomes more than 70% during July and August. One more potential player responsible for the higher AOD values during these months is the surface wind speed. Wind speed becomes stronger during this period and reaches almost >10 m s^{-1} (Fig. 7), which can significantly pick up the soil, dust and biological particles (which will be mostly in the coarse particle regime) and suspends in the atmosphere. In order to the support the above argument, aerosol fine mode fraction (FMF) from MODIS (Terra) has been analyzed for the study period (2002–2011) and its monthly mean variation is shown in Fig. 5. MODIS FMF, which is the ratio of the fine mode aerosol optical depth to the total aerosol optical depth, can be used as a proxy for delineating fine mode aerosols from coarse mode aerosols. From Fig. 5, it is clear that, with the increase of RH during monsoon months, the FMF decreased to reach a lower value of ~0.17. The least FMF value is recorded during May. Towards post-monsoon and winter months the FMF recovered to reach a maximum value of ~0.4 in December. The extensive rainfall during the months of September and October might have resulted in the significant washout of coarse mode aerosols, due to which the mean AOD values dropped to ~0.28. Winter months recorded the least AOD values over the study region, December AOD (~0.16 for Terra and 0.145 for Aqua) being the infimum. The very low temperature and relatively calm wind conditions during winter season might not have supported the generation of the aerosols through mechanical disintegrations processes.

4.3. Seasonal variations and long range transport

A Box plot for the seasonal variation of AOD (Terra and Aqua) for the study period is shown in Fig. 6, following the same conventions used for Fig. 4. The lowest seasonal mean Terra (Aqua) AOD value is recorded during winter with a value of $\sim 0.177 \pm 0.14$ (0.163 ± 0.13). The mean value increased towards summer reaching $\sim 0.291 \pm 0.17$ (0.3 ± 0.18) and attained peak in monsoon season with a value of $\sim 0.341 \pm 0.23$ (0.385 ± 0.23) and decreased during post-monsoon reaching as low as $\sim 0.268 \pm 0.17$ (0.276 ± 0.17).

Apart from the local emissions and modulations of the aerosol concentrations with respect to the synoptic meteorological conditions, long-range transport also contributes to the columnar aerosol load. The transport of natural and anthropogenic aerosols critically depends upon the synoptic scale circulation pattern. Wind vector plots and back trajectory analysis provide the information about the synoptic circulation pattern and potential pathways of transport. The season-wise mean synoptic wind pattern (at 850 h Pa) for the study period over the Indian subcontinent and surrounding regions is shown in Fig. 7. The isentropic trajectory cluster analysis at 1000 m agl typically for the year 2010 (within the study period) is shown in Fig. 8. During winter, the airmass/many of the trajectories reaching BNG are mostly from northern India, Indo-Gangetic plains (IGP) via Bay of Bengal (BoB), often trajectories reaching East Asian countries. North Indian region including the IGP is believed to be highly aerosol laden owing to its dense industrial and urban areas. On the north of Indian sub-continent, the orography of the Himalayas act as a natural boundary to the dispersion of aerosols and low temperature conditions in winter leads to the confinement and build-up of aerosols. The transported aerosol component from these regions might be rich in fine and accumulation mode (anthropogenic fraction). The FMF values obtained over BNG during winter are relatively high (with a seasonal mean of ~0.34) supporting the above argument. Towards summer, the study region experiences mixed airmass from east and west. From the figure it can be inferred that the airmass has both oceanic and continental history before reaching over to the study location. Summertime transport of the Arabian dust aerosol and associated lowering of columnar aerosol Angstrom exponent value has

Table 1
Month-wise AOD statistics.

Month	Mean AOD (550 nm)		Standard deviation		Number of data points		Minimum value		Maximum value	
	Terra	Aqua	Terra	Aqua	Terra	Aqua	Terra	Aqua	Terra	Aqua
January	0.170	0.145	0.134	0.125	231	200	0.002	0.002	0.8	0.853
February	0.204	0.190	0.167	0.157	225	194	0.001	0.005	0.939	0.948
March	0.253	0.251	0.161	0.168	239	221	0.002	0.002	0.856	0.829
April	0.294	0.326	0.167	0.188	247	220	0.005	0.008	0.904	0.944
May	0.327	0.333	0.187	0.181	247	207	0.004	0.021	1.201	1.03
June	0.306	0.322	0.225	0.210	132	104	0.003	0.010	1.174	0.983
July	0.399	0.474	0.227	0.245	69	69	0.016	0.030	1.09	1.004
August	0.352	0.395	0.240	0.232	85	82	0.02	0.118	1.183	1.014
September	0.260	0.271	0.185	0.171	142	129	0.007	0.019	0.977	0.928
October	0.277	0.280	0.156	0.178	155	176	0.011	0.011	0.761	0.931
November	0.173	0.178	0.120	0.110	169	163	0.001	0.002	0.777	0.562
December	0.161	0.145	0.127	0.109	214	208	0.003	0.001	0.845	0.652

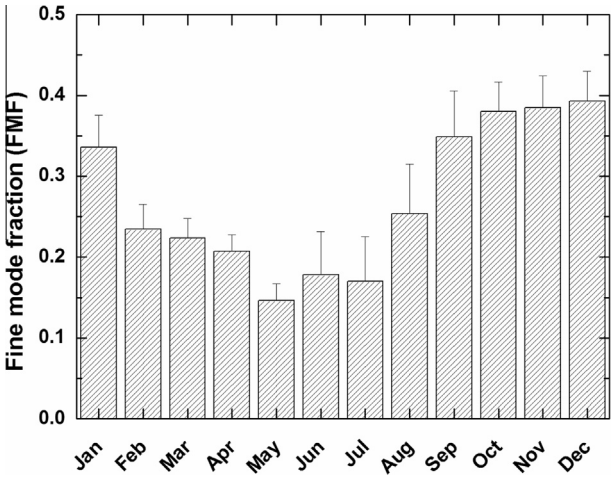

Fig. 5. Monthly mean variation of MODIS derived fine mode fraction (FMF) during the study period. Error bars represent the standard deviations.

been reported earlier over Indian sector (Niranjan et al., 2007). Therefore, it is difficult to arrive at a conclusion whether they bring in the marine/dust aerosol component over to the site, as in its transit it could pick up some anthropogenic aerosol over the continent. During summer, the moderate AOD values and low FMF values support this argument. The airmass reaching BNG during monsoon season is characterized by higher winds speeds (which was also evident by the lengthier trajectories) and long oceanic history over Arabian Sea and Indian Ocean. It is well known that the sea-salt production is strongly influenced by over-ocean winds and increase exponentially with wind speed (Moorthy et al., 1997). Also, the wind generated sea-spray aerosols will be in coarse size regime (Blanchard and Woodcock, 1980) and influence the size distribution parameters. In the present study, the higher AOD, standard deviation values during this season accompanied with lower values of FMF hint marine nature of aerosols over the study location. During post-monsoon, the study region experiences mixed airmass from Indian Ocean/Arabian Sea, Bay of Bengal via Indian subcontinent. During this

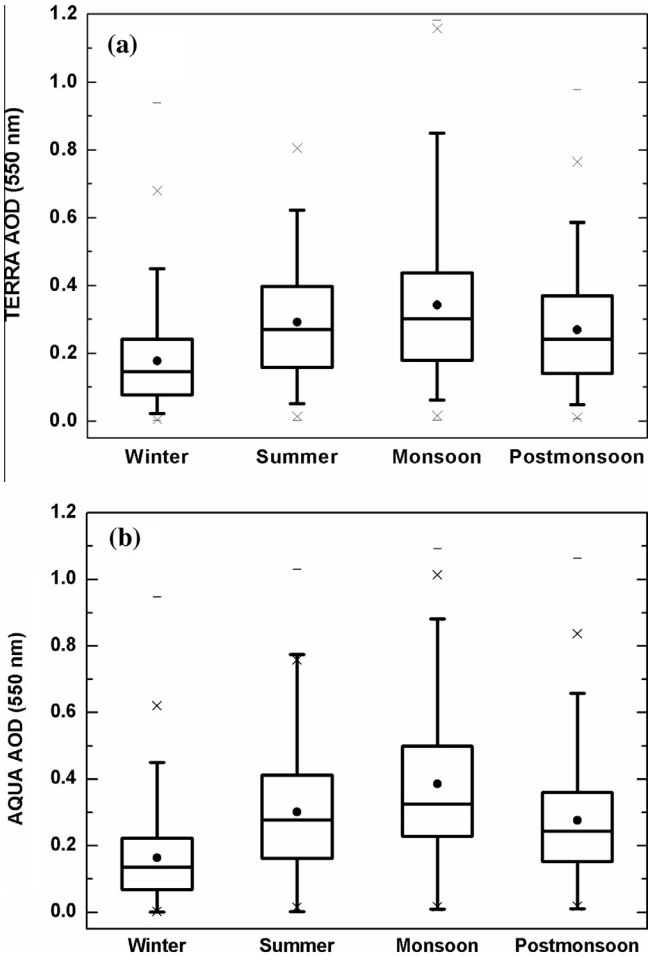

Fig. 6. Box plot for the seasonal variation of (a) Terra AOD; (b) Aqua AODover BNG. The conventions are same as that of Fig. 4.

season, the AOD values slightly dropped off, but the FMF values increased considerably nearing winter values.

4.4. Inter-annual variations

The inter-annual variations in the mean AOD (Terra and Aqua) during the study period are shown in Fig. 9.

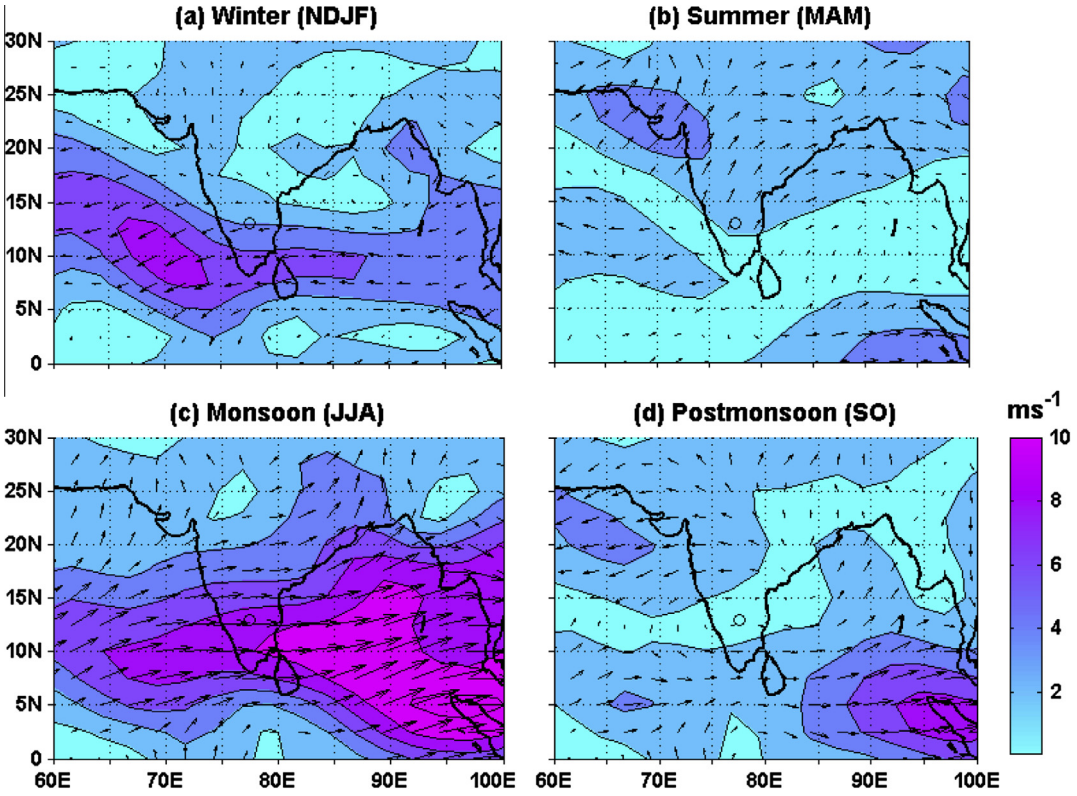

Fig. 7. Mean synoptic wind pattern at 850 h Pa for various seasons. Background color indicates the magnitude of the wind speed. Open circle represents the study location BNG.

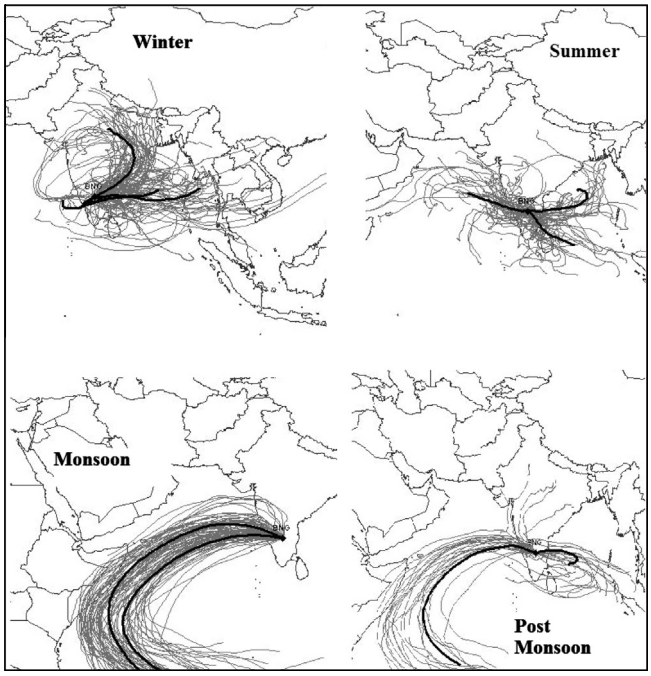

Fig. 8. Cluster analysis of seven day back trajectories at 1000 m above aground level arriving BNG for each of the seasons. Thick line represents the cluster mean.

The error bars in the figure represent the standard deviation from the mean value. The solid line represents the linear least square fit. The correlation coefficients are indicated on the respective plots. The climatological mean value of Terra (Aqua) AOD for the study period (2002–2011) is $\sim 0.253 \pm 0.2$ (0.281 ± 0.21). From the figure it is clear that annual mean AOD over BNG is exhibiting an increasing trend. From the linear least square fit, the estimated increase in Terra (Aqua) AOD value per year is ~ 0.005 (0.008). However, the observed trend is highly dependent on the monthly and yearly data and averaging aerosol properties over distinct length datasets can introduce biases in the trends (Kaskaoutis et al., 2012). The discrepancy in the number of (satellite/ground) observations per temporal interval highly depends on the presence of cloud and its seasonal variation, which in turn can lead to serious uncertainties in the trend analysis leading to problems with the statistical representativeness (Yoon et al., 2011). Hence, the trend in the AOD values has been re-estimated using median (instead of mean) values and weighted linear least squares regression as suggested by Kaskaoutis et al. (2012) and Yoon et al. (2012) respectively. The re-estimations yielded slope values of ~ 0.004 and ~ 0.002 for Terra AODs. For Aqua AODs the slopes are found to be ~ 0.007 and ~ 0.006 respectively. Further, the AOD trend has been estimated using seasonal mean values and the slopes are given in Table 3. The confidence level of the observed long term linear trend has been estimated by adopting the methodology given in Weatherhead et al. (1998). The ratio of standard deviation of the autoregressive noise in the linear fit to detected trend magnitude (for decade) for each of the fit has been computed. By comparing the obtained ratio with that of given in Table 1 of

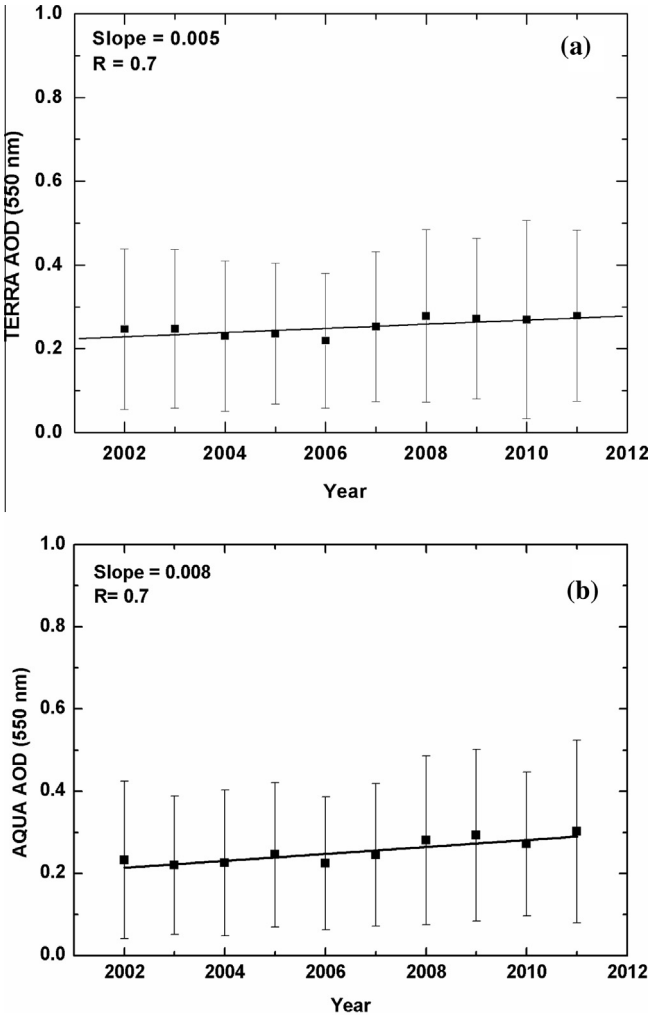

Fig. 9. Inter-annual variation of mean (a) Terra AOD; (b) Aqua AOD. Error bars indicate the standard deviation of the mean values. Solid line represents the linear least square fit.

Weatherhead et al. (1998), it has been inferred that 10 years of data (used in the present study) is adequate to detect the trend with 95% confidence level. From Table 3 it is clear that the increasing trend in the AOD values is mainly due to sustained increase in the seasonally averaged AOD values during the summer, followed by winter and then post-monsoon. This is true in case of both Terra and Aqua AODs. In contrast, a weak declining trend is observed in monsoon Terra AOD. These might be due to the fact that, during summer and winter seasons the trajectories reaching BNG have relatively longer history over the mainland compared to that of other two seasons, which can bring in more aerosols of continental origin. The rapid industrialization and the increase in the population also might be some of the reasons for the increase in AOD values over BNG. In the last decade (2001–2011) the population of BNG increased from ~5.1 to 8.5 million (~65%). In a recent study based on AERONET (during the period 2001–2010) measurements, Kaskaoutis et al. (2012) have shown an overall increase in AOD values on a yearly basis over Kanpur, Northern India. They also attributed the upward trend in AOD values (~0.0062 per year) to sustained increase in the seasonal/monthly averaged AOD during winter and post-monsoon seasons. They mentioned that their surface measurement based trends in AOD values are in agreement with those reported by satellite observations (MODIS and MISR) over northern India (Dey and Di Girolamo, 2011; Kaskaoutis et al., 2011). Ramachandran et al. (2012) based on ten years of MODIS level 2 data have also shown an increasing trend in the annual mean AOD values over most of the Indian locations including BNG. They reported an AOD growth of ~0.013 per year and ascribed it to increase in urbanization leading to an increase in the number of automobiles as BNG has emerged as a major high-tech city in the last decade.

4.5. Comparative study

The AOD values (at 550 nm) obtained over BNG in the present study are compared to that of other Indian locations having a variety of geographical, anthropogenic, climatic conditions. The comparison in shown in Table 2, all the stations and the corresponding data are arranged with increasing order of the latitude. As the classification of months to seasons is different for the different locations, the table is customized (started from the month of March) for a better understanding. All values pertaining to the table are derived from the ground based measurements using either Multi Wavelength Radiometer (Moorthy et al., 1997) or a part of AERONET (Holben et al., 1998) observations at 500 nm. Cosmopolitan cities like Hyderabad (HYD), Kanpur (KNP) recorded higher values of AOD compared to BNG during all the seasons. It is known that HYD, KNP are under the influence of the forest fires (Badarinath et al., 2007) and dust storms (Dey et al., 2004) respectively, though their strengths vary seasonally. Apart from the local activities the long range transported biomass burning aerosol and dust loading might be the reasons for the higher AODs over HYD and KNP. Even the coastal locations like Visakhapatnam (VSP, on the east coast) and Trivandrum (TVM, on the west coast) recorded higher AOD values compared to that of BNG. The monsoon season AOD over TVM is lower than that of BNG. The relatively higher rainfall distribution during the months of June–August might be the reason for the lower AOD value over TVM. Apart from the local anthropogenic activities and long-range transport, coastal locations are also influenced by the meso-scale circulation of the land and sea breeze activity. This circulation can bring in marine aerosol component onto the measurement locations during daytime and can increase the columnar aerosol load and thereby AOD. The semi-arid regions Anantapur (ATP), which is radially ~200 km from BNG, also recorded higher AOD values throughout the year when compared to that of BNG. The aerosol load over ATP is attributed to the industrial areas around, wind-blown dust due to the aridness of the region and transport

Table 2
Comparison of AOD values obtained in the present study with that of various Indian locations.

Location Lat., Long period reference	March	April	May	June	July	August	September	October	November	December	January	February
Bangalore (BNG) 13°N, 77.5°E 2002–2011 present study	0.291 ± 0.17 (Terra) 0.3 ± 0.18 (Aqua)			0.341 ± 0.23 (Terra) 0.385 ± 0.23 (Aqua)			0.268 ± 0.17 (Terra) 0.276 ± 0.17 (Aqua)		0.177 ± 0.14 (Terra)	0.163 ± 0.13 (Aqua)		
Bangalore (BNG) 13°N, 77.5°E 2001–2005 Vinoj et al. (2009)		0.5								0.2		
Trivandrum (TVM) (8.55°N, 76.97°E) 2000–2003 Moorthy et al. (2007)	0.4 ± 0.003			0.29 ± 0.03				0.38 ± 0.04		0.43 ± 0.01		
Port Blair (PBR) (11.63°N, 92.71°E) 2002 Moorthy et al. (2003)	–			–				–		–	0.29 ± 0.04	0.34 ± 0.03
Anantapur (ATP) (14.62°N, 77.65°E) 2005–2006 Kumar et al. (2009)	0.51 ± 0.21			0.46 ± 0.2						0.48 ± 0.18		
Hyderabad (HYD) (17.47°N, 78.43°E) 2007–2008 Kaskaoutis et al. (2009)	0.65 ± 0.32			0.568				0.46 ± 0.17		0.58		
Visakhapatnam (VSP) (17.7°N, 73.3°E) 2007 Niranjan et al. (2011)	0.58	0.59	0.65	0.5	–	0.46	0.4	0.55	0.34	0.46	0.49	0.44
Kanpur (KNP) (26.28°N, 80.2°E) 2001–2003 Singh et al. (2004)	0.54			0.66			0.63			0.57		
Dibrugarh (DBR) (27.3°N, 94.6°E) 2001–2007 (Gogoi et al., 2009)	0.45			0.25			0.19			0.31		
Nainital (NTL) (29.37°N, 79.45°E) 2004/2006 Pant et al. (2006) and Dumka et al. (2008)	0.09 ± 0.02	0.2 ± 0.04		–			–			–		0.059 ± 0.03
Patiala (PTL) (30.35°N, 76.54°E) 2006 Singh et al. (2008)	0.26 ± 0.08	0.36 ± 0.19	0.58 ± 0.2	–			–			–		

Table 3
Trend values of Terra and Aqua AOD over BNG during the period 2002–2011.

Trend estimation using	Trend/year	
	Terra AOD	Aqua AOD
Yearly mean	0.005	0.008
Yearly median	0.004	0.007
Weighted yearly mean (Yoon et al., 2012)	0.002	0.006
Winter season mean	0.003	0.007
Summer season mean	0.009	0.014
Monsoon season mean	−0.004	0.006
Post-monsoon season mean	0.002	0.006

(Kumar et al., 2009). The winter months mean AOD reported by Moorthy et al. (2003) over the island location Port Blair (over Bay of Bengal) is also higher than that of BNG. Coming to the north eastern location Dibrugarh (DBR), the summer and winter season AOD values are higher and the rest of the seasons are lower compared to BNG. Gogoi et al. (2009) inferred that the peculiar topography combined with the local conditions and the widespread rainfall lead to a more pristine environment during monsoon and retreating monsoon seasons which in turn lead to lower AOD values. The contrasting rainfall distribution pattern over DBR and BNG plays one of the key roles for the observed spatial heterogeneity in the AOD values. The pre-monsoon/summer months mean AOD reported by Singh et al. (2008) over Patiala (PTL) is comparatively higher than the summer season mean over BNG. PTL being located in the agrarian region of Northwest India, is close to Shivalik Hills in the east and Thar Desert in the Southwest. Singh et al. (2008) attributed the increase in the AOD towards the later months of summer to the transported dust by southerly winds. Pant et al. (2006) reported a very low value of winter time AOD (~0.059) for Manora Peak, Nainital (NTL), which is a high-altitude station (~1950 m amsl) in the central Himalayas. Even though BNG is also located at an altitude of ~900 m amsl, due to its urban, industrial and cosmopolitan nature, the AOD values at BNG are far high compared to NTL.

4.6. Radiative and climate impacts

The importance of atmospheric aerosols is being increasingly recognized in recent years in the regional and global radiative forcing and the resulting climatic implications (Charlson et al., 1992). Aerosols play a vital role in the Earth–atmosphere–ocean system by means of their direct and indirect impact on climate (Schwartz et al., 1995). Recent studies have shown that the surface and/or column integrated aerosol measurements alone are inadequate to assess aerosol induced climate changes (e.g. Satheesh et al., 2010). The information on vertical distribution of aerosols is essential to address complex problems such as radiative impact of aerosols and to estimate altitude profiles of aerosol-induced warming. Satheesh (2002)

has demonstrated that, depending on the relative altitude of the aerosol layer and the clouds, the aerosol forcing can vary significantly for the same aerosol concentration and composition. The vertical distribution of aerosol chemical species also plays a vital role in the aerosol radiative forcing. Absorbing aerosols such as black carbon if located above (scattering) clouds result in enhanced absorption, than if they were present over dark ocean surfaces (Chand et al., 2009).

Satheesh et al. (2008) have shown that during pre-monsoon/summer season most of the Indian landmass is characterized by elevated aerosol layers. Over south central India during pre-monsoon, they reported that ~50–70% of AOD was found contributed by aerosols above reflecting clouds. Note that the present study location BNG comes under the south central Indian region. The impact of the elevated aerosols in the advancement and intensification of Indian summer monsoon has been clearly demonstrated by Lau et al. (2006). Satheesh et al. (2008) have indicated the possibility of the elevated heat pump (EHP, demonstrated by Lau et al. (2006)) effect over most of Indian subcontinent and adjoining oceans during pre-monsoon. Using ground based measurements and modeling studies, Satheesh et al. (2010) have estimated the regional radiative forcing over BNG and reported surface radiative forcing (reduction in the ground reaching solar irradiance) values varying from 30 to 65 W m^{-2} during winter to summer. In the present study it is observed that the annual mean AOD value over BNG increases year to year. Heavy aerosol loading in the atmosphere can have both hydrological and radiative cloud-mediated effects on the climate (Andreae et al., 2005). Apart from the direct aerosol radiative effects, aerosols through their indirect effects can modulate the precipitation over a region by acting as cloud condensation nuclei (CCN). Many observational studies of aerosol indirect effects (e.g. Rosenfeld and Lensky, 1998) have shown aerosols either suppress or enhance precipitation. In a recent airborne study by Konwar et al. (2010) over Indian subcontinent, they have shown that the pollution aerosols redistribute the rainfall such that less rainfall occurs in areas where rain amounts are modest anyway, and more rainfall occurs where it already rains heavily. Rosenfeld (2000) demonstrated that urban and industrial air pollution can completely shut off precipitation from clouds that have temperatures at their tops of about −10 °C. The suppression of the precipitation due to continuous build up of aerosol load can still lower the strength of the aerosol wet deposition mechanism. This in turn can aid the aerosol accumulation over a region. This process can be treated as a positive feedback mechanism, which can result in a drought like situation.

5. Conclusions

Ten years (2002–2011) MODIS aerosol optical depths (AOD at 550 nm) have been analyzed to delineate the temporal variations in the aerosol columnar optical properties over Bangalore, India. The major conclusions drawn out of the study are

1. Terra and Aqua AODs exhibited similar temporal variation patterns.
2. AOD exhibited large temporal variations on monthly and seasonal scales. The minimum monthly mean Terra AOD is observed during December with a value of $\sim 0.161 \pm 0.12$ and the maximum value is observed during July with a mean value of $\sim 0.399 \pm 0.22$.
3. Season-wise, the minimum value in Terra AOD is observed during winter ($\sim 0.177 \pm 0.14$) and the maximum value during monsoon ($\sim 0.341 \pm 0.23$).
4. The observed AOD values are lower compared to the other urban, coastal locations over Indian subcontinent and higher compared to the high altitude Himalayan station.
5. The annual mean and median Terra AOD values have shown an increasing trend at a rate of ~0.005 and ~0.004 per year respectively with 95% confidence level.

Acknowledgements

The data used in this study are downloaded using the GES-DISC Interactive Online Visualization and Analysis Infrastructure, a part of the NASA's Goddard Earth Sciences Data and Information Services Center. Synoptic wind patterns have been computed using NCEP/NCAR reanalysis data. The author acknowledges the constructive comments and suggestion of the two anonymous reviewers. The trajectories are computed using NOAA HYSPLIT model.

Appendix A. Supplementary data

Supplementary data associated with this article can be found, in the online version, at http://dx.doi.org/10.1016/j.asr.2013.01.022.

References

Andreae, M.O., Jones, C.D., Cox, P.M. Strong present-day aerosol cooling implies a hot future. Nature 435, 1187–1190, 2005.

Babu, S.S., Satheesh, S.K., Moorthy, K.K. Aerosol radiative forcing due to enhanced black carbon at an urban site in India. Geophys. Res. Lett. 29 (18), 1880, http://dx.doi.org/10.1029/2002GL015826, 2002.

Badarinath, K.V.S., Kharol, S.K., Kaskaoutis, D.G., Kambezidis, H.D. Influence of atmospheric aerosols on solar spectral irradiance in an urban area. J. Atmos. Sol. Terr. Phys. 69, 589–599, http://dx.doi.org/10.1016/j.jastp. 2006.10.010, 2007.

Blanchard, D.C., Woodcock, A.H. The production, concentration, and vertical distribution of the sea-salt aerosol. Ann. N. Y. Acad. Sci. 338, 330–347, 1980.

Chand, D., Wood, R., Anderson, T.L., Satheesh, S.K., Charlson, R.J. Satellite-derived direct radiative effect of aerosols dependent on cloud cover. Nat. Geosci. 2, 181–184, http://dx.doi.org/10.1038/ngeo437, 2009.

Charlson, R.J., Schwartz, S.E., Hales, J.M., Cess, R.D., Coakley Jr, J.A., Hansen, J.E., Hofmann, D.J. Climate forcing by anthropogenic aerosols. Science 255, 423–430, 1992.

Choudhry, P., Misra, A., Tripathi, S.N. Study of MODIS derived AOD at three different locations in the Indo Gangetic Plain: Kanpur, Gandhi College and Nainital. Ann. Geophys. 30, 1479–1493, 2012.

Dey, S., Tripathi, S.N., Singh, R.P., Holben, B.N. Influence of dust storms on aerosol optical properties over the Indo-Gangetic basin. J. Geophys. Res. 109, D20211, http://dx.doi.org/10.1029/2004JD004924, 2004.

Dey, S., Di Girolamo, L. A decade of change in aerosol properties over the Indian subcontinent. Geophys. Res. Lett. 38, L14811, 2011.

Dimitrova, R., Lurponglukana, N., Fernando, H.J.S., Runger, G.C., Hyde, P., Hedquist, B.C., Anderson, J., Bannister, W., Johnson, W. Relationship between particulate matter and childhood asthma – basis of a future warning system for central Phoenix. Atmos. Chem. Phys. 12, 2479–2490, http://dx.doi.org/10.5194/acp-12-2479-2012, 2012.

Dumka, U.C., Moorthy, K.K., Pant, P., Hegde, P., Sagar, R., Pandey, K. Physical and optical characteristics of atmospheric aerosolsduring ICARB at Manora Peak, Nainital: a sparsely inhabited, high-altitude location in the Himalayas. J. Earth Syst. Sci. 117 (S1), 399–405, 2008.

Eck, T.F., Holben, D.N., Dubovik, O., Smirnov, A., Slutsker, I., Lobert, J.M., Ramanathan, V. Column-integrated aerosol optical properties over the Maldives during the northeast monsoon for 1998–2000. J. Geophys. Res. 106 (28), 555–566, 2001.

Gogoi, M.M., Moorthy, K.K., Babu, S.S., Bhuyan, P.K. Climatology of columnar aerosol properties and the influence of synoptic conditions: first-time results from the northeastern region of India. J. Geophys. Res. 114, D08202, http://dx.doi.org/10.1029/2008JD010765, 2009.

Guinot, B., Cachier, H., Sciare, J., Tong, Y., Xin, W., Jianhua, Y. Beijing aerosol: atmospheric interactions and new trends. J. Geophys. Res. 112, D14314, http://dx.doi.org/10.1029/2006JD008195, 2007.

Holben, B.N. et al. AERONET-a federated instrument network and data archive for aerosol characterization. Remote Sens. Environ. 66, 1–16, 1998.

Jethva, H., Satheesh, S.K., Srinivasan, J. Assessment of second generation MODIS aerosol retrieval (Collection 005) at Kanpur, India. Geophys. Res. Lett. 34, L19802, http://dx.doi.org/10.1029/2007GL029647, 2007.

Kaskaoutis, D.G., Kharol, S.K., Sinha, P.R., Singh, R.P., Badarinath, K.V.S., Mehdi, W., Sharma, M. Contrasting aerosol trends over South Asia during the last decade based on MODIS observations. Atmos. Meas. Tech. Discuss. 4, 5275–5323, 2011.

Kaskaoutis, D.G., Badarinath, K.V.S., Kharol, S.K., Sharma, A.R., Kambezidis, H.D. Variations in the aerosol optical properties and types over the tropical urban site of Hyderabad, India. J. Geophys. Res. 114, D22204, http://dx.doi.org/10.1029/2009JD012423, 2009.

Kaskaoutis, D.G., Singh, R.P., Gautam, R., Sharma, M., Kosmopoulos, P.G., Tripathi, S.N. Variability and trends of aerosol properties over Kanpur, Northern India using AERONET data (2001–2010). Environ. Res. Lett. 7, 024003, 2012.

Kaufman, Y.J., Tanré, D., Remer, L.A., Vermote, E.F., Chu, A., Holben, B.N. Operational remote sensing of tropospheric aerosol over land from EOS moderate-resolution imaging spectroradiometer. J. Geophys. Res. 102, 17, 051–17, 065, http://dx.doi.org/10.1029/96JD03988, 1997.

Konwar, M., Maheskumar, R.S., Kulkarni, J.R., Freud, E., Goswami, B.N., Rosenfeld, D. Suppression of warm rain by aerosols in rain-shadow areas of India. Atmos. Chem. Phys. Discuss. 10, 17009–17027, http://dx.doi.org/10.5194/acpd-10-17009-2010, 2010.

Kumar, K.R., Narasimhulu, K., Reddy, R.R., Gopal, K.R., Reddy, L.S.S., Balakrishnaiah, G., Moorthy, K.K., Babu, S.S. Temporal and spectral characteristics of aerosol optical depths in a semi-arid region of Southern India. Sci. Tot. Environ. 407, 2673–2688, http://dx.doi.org/10.1016/j.scitotenv.2008.10.028, 2009.

Lau, K.M., Kim, M.K., Kim, K.M. Asian monsoon anomalies induced by aerosol direct forcing: the role of the Tibetan Plateau. Clim. Dyn. 26, 855–864, http://dx.doi.org/10.1007/s00382-006-0114-z, 2006.

Lawrence, M.G., Lelieveld, J. Atmospheric pollutant outflow from Southern Asia: a review. Atmos. Chem. Phys. 10, 11017–11096, 2010.

Levy, R.C., Remer, L.A., Tanré, D., Kaufman, Y.J., Ichoku, C., Holben, B.N., Livingston, J.M., Russell, P.B., Maring, H. Evaluation of the moderate-resolution imaging spectroradiometer (MODIS) retrievals of dust aerosol over the ocean during PRIDE. J. Geophys. Res. 108 (D19), 8594, http://dx.doi.org/10.1029/2002JD002460, 2003.

Levy, R., Remer, L.A., Mattoo, S., Vermote, E., Kaufman, Y.J. Second generation algorithm for retrieving aerosol properties over land from MODIS spectral reflectance. J. Geophys. Res. 112, D13211, http://dx.doi.org/10.1029/2006JD007811, 2007.

Moorthy, K.K., Satheesh, S.K., Murthy, B.V.K. Investigation of marine aerosols over the tropical Indian Ocean. J. Geophys. Res. 102, 18, 827–18, 842, 1997.

Moorthy, K.K., Babu, S.S., Satheesh, S.K. Aerosol spectral optical depths over the Bay of Bengal: role of transport. Geophys. Res. Lett. 30 (5), 1249, http://dx.doi.org/10.1029/2002GL016520, 2003.

Moorthy, K.K., Babu, S.S., Satheesh, S.K. Temporal heterogeneity in aerosol characteristics and the resulting radiative impact at a tropical coastal station – Part 1: Microphysical and optical properties. Ann. Geophys. 25, 2293–2308, 2007.

Niranjan, K., Madhavan, B.L., Sreekanth, V. Micro pulse LIDAR observation of high altitude aerosol layers at Visakhapatnam located on the east coast of India. Geophys. Res. Lett. 34, L03815, http://dx.doi.org/10.1029/2006GL028199, 2007.

Niranjan, K., Spandana, B., Devi, T.A., Sreekanth, V., Madhavan, B.L. Measurements of aerosol intensive properties over Visakhapatnam, India for 2007. Ann. Geophys. 29 (973–985), 2011, 2011.

Pant, P., Hegde, P., Dumka, U.C., Sagar, R., Satheesh, S.K., Moorthy, K.K., Saha, A., Srivastava, M.K. Aerosol characteristics at a high-altitude location in central Himalayas: optical properties and radiative forcing. J. Geophys. Res. 111, D17206, http://dx.doi.org/10.1029/2005JD006768, 2006.

Ramachandran, S., Cherian, R. Regional and seasonal variations in aerosol optical characteristics and their frequency distributions over India during 2001–2005. J. Geophys. Res. 113, D08207, http://dx.doi.org/10.1029/2007JD008560, 2008.

Ramachandran, S., Kedia, S., Srivastava, R. Aerosol optical depth trends over different regions of India. Atmos. Environ. 49, 338–347, 2012.

Remer, L.A. et al. The MODIS aerosol algorithm, products and validation. J. Atmos. Sci. 62 (4), 947–973, http://dx.doi.org/10.1175/JAS3385.1, 2005.

Remer, L.A., Kleidman, R.G., Levy, R.C., Kaufman, Y.J., Tanré, D., Mattoo, S., Martins, J.V., Ichoku, C., Koren, I., Yu, H., Holben, B.N. Global aerosol climatology from the MODIS satellite sensors. J. Geophys. Res. 113, D14S07, http://dx.doi.org/10.1029/2007JD009661, 2008.

Rosenfeld, D. Suppression of rain and snow by urban and industrial air pollution. Science 287 (5459), 1793–1796, 2000.

Rosenfeld, D., Lensky, I. Satellite-based insights into precipitation formation processes in continental and maritime convective clouds. Bull. Am. Meteorol. Soc. 79, 2457–2476, 1998.

Satheesh, S.K. Aerosol radiative forcing over land: effect of surface and cloud reflection. Ann. Geophys. 20, 2105–2109, 2002.

Satheesh, S.K., Vinoj, V., Moorthy, K.K. Vertical distribution of aerosols over an urban continental site in India inferred using a micro pulse LIDAR. Geophys. Res. Lett. 33, L20816, http://dx.doi.org/10.1029/2006GL027729, 2006.

Satheesh, S.K., Moorthy, K.K., Babu, S.S., Vinoj, V., Dutt, C.B.S. Climate implications of large warming by elevated aerosol over India. Geophys. Res. Lett. 35, L19809, http://dx.doi.org/10.1029/2008GL034944, 2008.

Satheesh, S.K., Vinoj, V., Moorthy, K.K. Radiative effects of aerosols at an urban location in Southern India: observations versus model. Atmos. Environ. 44, 5295–5304, 2010.

Schwartz, S.E. et al. Group Report: Connections between Aerosol Properties and Forcing of Climate. John Wiley, Hoboken, 1995.

Singh, R.P., Dey, S., Tripathi, S.N., Tare, V. Variability of aerosol parameters over Kanpur; Northern India. J. Geophys. Res. 109, D23206, http://dx.doi.org/10.1029/2004JD004966, 2004.

Singh, M., Singh, D., Pant, P. Aerosol characteristics at Patiala during ICARB–2006. J. Earth Syst. Sci. 117 (S1), 407–411, 2008.

Smirnov, A. et al. Maritime aerosol network as a component of aerosol robotic network. J. Geophys. Res. 114, D06204, http://dx.doi.org/10.1029/2008JD011257, 2009.

Tanré, D., Kaufman, Y.J., Herman, M., Mattoo, S. Remote sensing of aerosol properties over oceans using the MODIS/EOS spectral radiances. J. Geophys. Res. 102, 971–988, http://dx.doi.org/10.1029/96JD03437, 1997.

Vinoj, V., Satheesh, S.K., Babu, S.S., Moorthy, K.K. Large aerosol optical depths observed at an urban location in southern India associated with rain-deficit summer monsoon season. Ann. Geophys. 22, 3073–3077, 2004.

Vinoj, V., Satheesh, S.K., Moorthy, K.K. Aerosol characteristics at a continental urban station in Southern India. Int. J. Environ. Waste Manage. 4 (1/2), 256–266, 2009.

Weatherhead, E.C., Reinsel, G.C., Tiao, G.C., Meng, X.-L., Choi, D., Cheang, W.-K., Keller, T., DeLuisi, J., Wuebbles, D.J., Kerr, J.B., Miller, A.J., Oltmans, S.J., Frederick, J.E. Factors affecting the detection of trends: statistical considerations and applications to environmental data. J. Geophys. Res. 103, 17149–17161, http://dx.doi.org/10.1029/98JD00995, 1998.

Yoon, J., von Hoyningen-Huene, W., Vountas, M., Burrows, J.P. Analysis of linear long-term trend of aerosol optical thickness derived from SeaWiFS using BAER over Europe and South China. Atmos. Chem. Phys. 11, 12149–12167, http://dx.doi.org/10.5194/acp-11-12149-2011, 2011.

Yoon, J., von Hoyningen-Huene, W., Kokhanousky, A.A., Vountas, M., Burrows, J.P. Trend analysis of aerosol optical thickness and Angstrom exponent derived from the global AERONET spectral observations. Atmos. Meas. Tech. 5, 1271–1299, 2012.

Yu, H., Chin, M., Winker, D.M., Omar, A.H., Liu, Z., Kittaka, C., Diehl, T. Global view of aerosol vertical distributions from CALIPSO LIDAR measurements and GOCART simulations: regional and seasonal variations. J. Geophys. Res. 115, D00H30, http://dx.doi.org/10.1029/2009JD013364, 2010.

Xin, J., Wang, S., Wang, Y., Yuan, J., Zhang, W., Sun, Y. Optical properties and size distribution of dust aerosols over the Tengger Desert in Northern China. Atmos. Environ. 39, 5971–5978, http://dx.doi.org/10.1016/j.atmosenv.2005.06.027, 2005.